Probing the Interaction of Magnetic Iron Oxide Nanoparticles with Bovine Serum Albumin by Spectroscopic Techniques

Qinqin Yang,† Jiangong Liang,† and Heyou Han*

College of Science, State Key Laboratory of Agricultural Microbiology, Institute of Chemical Biology, Huazhong Agricultural University, Wuhan, 430070, People's Republic of China

Received: April 30, 2009; Revised Manuscript Received: June 10, 2009

The interaction of magnetic iron oxide nanoparticles (MNPs) with bovine serum albumin (BSA) was investigated by fluorescence (FL), ultraviolet visible (UV−vis) absorption, Raman, and circular dichroism (CD) spectroscopy. Results indicated that MNPs quench BSA FL mainly by a static quenching mechanism. The FL quenching constants K_{SV} were obtained as 2.44×10^8, 2.41×10^8, and 2.40×10^8 L·mol^{-1} at 291, 298, and 313 K, respectively. The thermodynamic parameters of enthalpy change ΔH^θ, entropy change ΔS^θ, and free energy change ΔG^θ were −0.90 kJ·mol^{-1}, 157.38 J·mol^{-1}·K^{-1}, and −47.80 kJ·mol^{-1} (298 K), respectively. The association constant (K_A) and the number of binding sites (n) were 7.64×10^7 L·mol^{-1} and 46.55 at higher concentration of MNPs, and 1.35×10^6 L·mol^{-1} and 284.74 at lower concentration of MNPs. The analysis results suggested that the interaction was spontaneous and the electrostatic interactions played key roles in the reaction process. In addition, the Raman and CD spectra proved secondary structure alteration of BSA in the presence of MNPs.

1. Introduction

Magnetic iron oxide nanoparticles (MNPs) have shown great prospect in a wide variety of biological and biomedical applications such as cellular labeling, molecular imaging, in vitro bioseparation, and drug delivery[1] owing to their unique magnetic properties and biocompatibility. However, little is known about their potential adverse effects on health due to prolonged exposure in biological systems, which is a bottleneck to the development of MNPs on nanobiology, nanomedicine, and nanotoxicology. In particular, the behavior of MNPs inside the cells is still an enigma. The metabolic and immunological responses induced by these particles have been rarely understood so far.[2]

Recently, there have been some reports about toxicity of MNPs on cell. Pisanic et al. demonstrated that exposure to the increasing concentrations of anionic magnetic nanoparticles results in a dose-dependent diminishing viability and capacity of PC12 cells.[3] Another microscopic study by Jeng et al. determined that nanoparticle-exposed Neuro-2A cells at doses higher than 100 mg·mL^{-1} became abnormal in size, displaying cellular shrinkage, and detachment. Fe_3O_4 had measurable effect on the cells when the concentrations were greater than 200 mg·mL^{-1}.[4] Y. Q. Wang et al. studied the effect of colloidal Fe_3O_4 on the conformation of BHb by traditional spectroscopic techniques, including UV−vis, FT-IR, FL, resonance light scattering spectra, circular dichroism, synchronous FL, and three-dimensional FL spectra.[5] Nevertheless, intensive research on mechanism of MNPs with other proteins is still meaningful and the effect of MNPs on other proteins is worth further studies.

Our report described a detailed investigation on mechanism of MNPs bound to a model biological host (bovine serum albumin). Bovine serum albumin (BSA) has been one of the most extensively studied proteins, particularly thanks to its structural homology with human serum albumin (HSA).[6,7] It is a small protein with a single polypeptide chain, which is cross-linked by 17 disulfide bonds.[8,9] In the present study, the interaction of MNPs and BSA were mainly investigated with FL spectra at 291, 298, and 306 K. The FL quenching constants, quenching rate constant, association constant, number of binding sites, and thermodynamic parameters of the interaction were calculated, by which we found there was a strong static quenching and primary electrostatic interaction between the MNPs and BSA. Two different binding modes were found at different concentrations of MNPs, which were different from the outcome of Wang et al.[5] In addition, the mechanism of the reaction was further estimated by Raman and CD spectra which demonstrated that MNPs indeed effect the conformation of BSA. The findings of this paper will not only have significance on the toxicity of MNPs and the binding mode of MNPs and proteins but also provide important evidence for the application of MNPs in biological markers, molecular probe, medical diagnosis, and other fields.

2. Experimental Procedures

2.1. Materials. $FeSO_4 \cdot 7H_2O$, $FeCl_3 \cdot 6H_2O$, 25% aqueous ammonia, 35% hydrochloric acid, acetone, and dodecanebenzenesulfonic acid sodium salt were obtained from Sinopharm Chemical Reagent Co., Ltd. (Shanghai, China). Oleic acid was obtained from Tianjin Guangfu Fine Chemical Research Institute (Tianjin, China). And BSA was purchased from Shanghai Boao Biochemical Technology Co. (Shanghai, China,). All other chemicals were of analytical grade and were used without further purification.

2.2. Apparatus. The size of MNPs was acquired with a JEOL-JEM-2010 transmission electron microscope (JEOL/NTC., Japan). Powder X-ray diffraction was recorded using a D/Max-3B X-ray diffractometer (Rigaku International Corp., Japan) with Fe Kα source (36 kV and 20 mA). The weight loss of the MNPs was recorded by a TG209 thermogravimetric anylyzer (Netzsch, German). The UV−vis absorption spectra

* Corresponding author. Phone: 0086-(0)27 87288246. Fax: 0086-(0)27 87288246. E-mail: hyhan@mail.hzau.edu.cn.
† Equal contribution by the first two authors.

10.1021/jp904004w CCC: $40.75
Published on Web 07/07/2009

SCHEME 1: Schematic Representation of Ligand Exchange Process (path A) and Interaction with BSA (path B) of MNPs

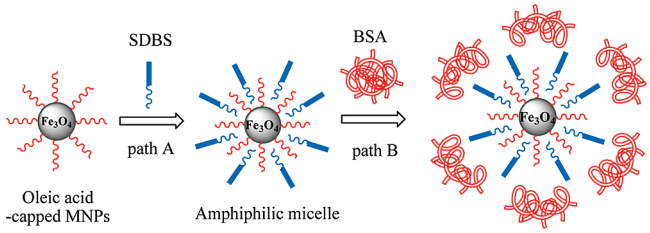

were obtained in the range of 190−700 nm, with 1.0 cm × 1.0 cm quartz cuvette on a Thermo Nicolet Corp. model Evolution 300 (America). All FL spectra were recorded by a Perkin-Elmer LS-55 FL spectrometer (America) equipped with a 20 kW xenon discharge lamp as a light source. The Raman spectra were acquired with an inVia micro-Raman spectroscopy system (Renishow, UK) in a spectral range of 300−2000 cm^{-1}, equipped with a He−Ne laser excitation source emitting wavelength at 633 nm. The CD spectra were carried out in a J-810 circular dichroism chiroptical spectrometer (Jasco, Japan), with wavelengths ranging from 190 to 300 nm, by using a cell with a path length of 0.1 cm. All pH measurements were tested with a Model MP120 pH meter (Mettler-Toledo Instruments Ltd., Swiss).

2.3. Synthesis and Characterization of MNPs. MNPs were synthesized following the method described in the literature with some modifications.[10] Briefly, 1.39 g of $FeSO_4 \cdot 7H_2O$ and 2.70 g of $FeCl_3 \cdot 6H_2O$ were added to flask with constant stirring. The initial pH of the iron salts mixture was adjusted to 1.5 and was digested for 30 min. Then, the pH was increased rapidly (within 20 s) to 10 by adding 25% of aqueous ammonia at constant rate. After 30 min of digestion, addition of 9.5 mL of oleic acid was carried out dynamically at 70 °C for 30 min. The as-prepared particles were initially washed with acetone for the removal of ionic impurities, and then dried at room temperature in inert atmosphere.

The dried particles were transferred to aqueous phase by dispersing them in 0.003 mol·L^{-1} dodecanebenzenesulfonic acid sodium salt solution[11] (Scheme 1, path A).

2.4. Probing the Interaction between MNPs and BSA. 2.5 mL of 0.05 mol·L^{-1} Tris-HCl buffer at pH 7.4, 4.0 × 10^{-7} mol·L^{-1} of MNPs, 0.003 mol·L^{-1} of SDBS, and 0.5 mL 1.0 × 10^{-5} mol·L^{-1} of BSA were transferred to 5.00 mL comparison tubes in sequence. BSA and total SDBS concentration were fixed at 1.0 × 10^{-6} and 3.0 × 10^{-4} mol·L^{-1}, respectively. The concentrations of MNPs were varied from 0 to 4.0 × 10^{-8} mol·L^{-1}. FL spectra were recorded at 291, 298, and 306 K in the range of 290−450 nm upon excitation at 280 nm in each case. The excitation and emission slit widths were fixed at 15.0 and 2.5 nm.

3. Results and Discussion

3.1. Characterization of As-Prepared MNPs. Figure 1 shows the TEM image of the MNPs. It can be seen that the distribution of size was narrow and the particle average diameters of the as-prepared MNPs are around 9.2 nm. Figure S1 in the Supporting Information displays the XRD pattern of MNPs. The peaks with 2θ values of 22.78°, 37.88°, 44.84°, 54.66°, 68.44°, 73.46°, and 81.44° correspond to the crystal planes (111), (220), (311), (400), (422), (511), and (440)[12] of cubic crystal structure Fe_3O_4. The peak positions and relative intensities of nanoparticles are consistent with XRD patterns

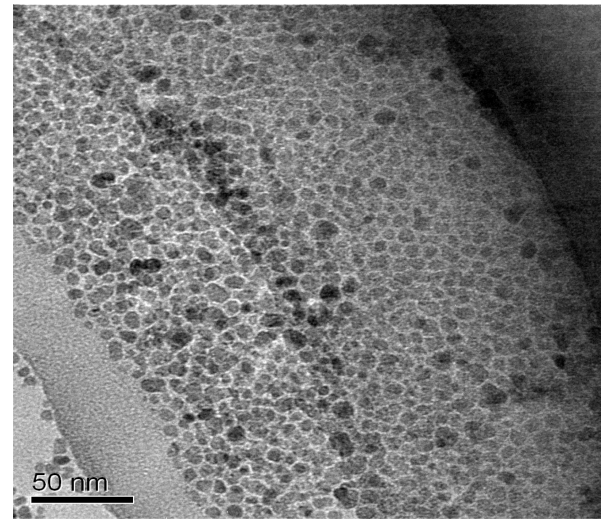

Figure 1. TEM image of oleic acid-capped MNPs.

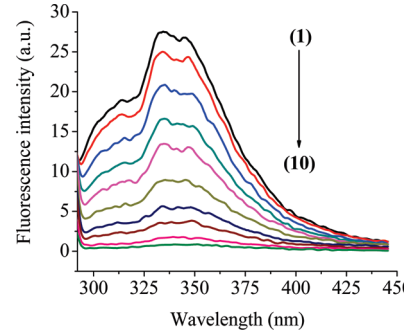

Figure 2. FL spectra of BSA in the presence of MNPs. BSA concentration was fixed at 1.0 × 10^{-6} mol·L^{-1}. MNPs concentrations were (1) 0, (2) 0.4, (3) 1.6, (4) 3.2, (5) 4.8, (6) 8.0, (7) 12, (8) 16, (9) 24, and (10) 32 (×10^{-9} mol·L^{-1}), respectively.

of standard Fe_3O_4, which confirmed the inverse spinel structure of the magnetite materials.[13] The TGA analyses (Figure S2, Supporting Information) showed that the total weight loss of the as-prepared MNPs was 29.3%.

3.2. Thermodynamic Study on the Interaction. ***3.2.1. Effect of BSA Concentration.*** FL quenching is a process which decreases the intensity of the FL emission. The effect of MNPs on BSA FL intensity is depicted in Figure 2. When different amounts of MNPs were added to a fixed concentration of BSA, a remarkable decrease in the FL intensity of BSA was observed, indicating a strong interaction between BSA and MNPs.

The FL quenching data were analyzed by the Stern−Volmer equation:[14]

$$F_0/F = 1 + K_{SV}[Q] = 1 + K_q\tau_0[Q] \quad (1)$$

where F_0 and F denote FL intensities of BSA in the absence and presence of MNPs, respectively, K_{SV} is the Stern−Volmer quenching constant and [Q] is the concentration of MNPs. The plot of F_0/F versus [Q] (Figure 3) showed a positive deviation (concave toward the y axis), indicating the presence of both static and dynamic quenching.[15] Since the FL lifetime of the biopolymer was 10^{-8} s,[16] the quenching rate constant, K_q, could be calculated according to equation $K_q = K_{SV}/\tau_0$. The maximum diffusion collision rate constant of various quenchers with the biopolymer was 2.0 × 10^{10} L·mol^{-1}·s^{-1}. This K_q value was observed to be 2.41 × 10^{16} L·mol^{-1}·s^{-1} at 298 K. The

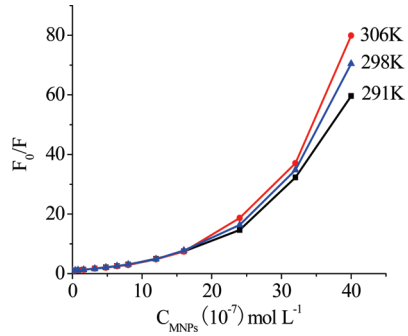

Figure 3. Unmodified Stern−Volmer curves of F_0/F vs concentration of MNPs at different temperature. The concentration of BSA was 1.0 × 10^{-6} mol·L^{-1}.

TABLE 1: Modified Stern−Volmer Equations for Interaction of MNPs with BSA at Different Temperatures

T/K	linear equation	f_a	K_{SV}/(×10^8 L·mol^{-1})	K_q/(×10^{16} L·mol^{-1}·s^{-1})	r
291	$F_0/(F_0 - F) = 1.06 + 4.09 \times 10^{-9}[Q]^{-1}$	0.941	2.44	2.44	0.9887
298	$F_0/(F_0 - F) = 1.03 + 4.15 \times 10^{-9}[Q]^{-1}$	0.968	2.41	2.41	0.9970
306	$F_0/(F_0 - F) = 1.06 + 4.17 \times 10^{-9}[Q]^{-1}$	0.939	2.40	2.40	0.9935

quenching rate constants at different temperatures (Table 1) were much greater than those in the biopolymer (2.0 × 10^{10} L·mol^{-1}·s^{-1}). Consequently, the quenching was probably initiated by the formation of a complex instead of dynamic collision.[8]

UV−vis absorption is a simple and applicable measurement to explore the structural changes and prove the complex formation.[8,17] As shown in Figure 4a, there was a strong absorption band at around 230 nm which was mainly due to the transition of P → P* of BSA's characteristic polypeptide backbone structure C═O.[18] When MNPs was added, the UV−vis absorbance (Figure 4d) was obviously different from the sum of the absorbance of BSA (Figure 4a) and MNPs (Figure 4b). The conformational changes reflected by the spectral difference at 230 nm in the UV−vis spectra might arise from disturbances of polypeptide's environment of the protein.[19,20]

In the case of static or dynamic quenching process, the quenching constant (K_{SV}) of BSA was determined from the Stern−Volmer equation modified by Lehrer:[21]

$$F_0/(F_0 - F) = 1/f_a + 1/(K_{SV}[Q]) \quad (2)$$

F_0 and F are the relative FL of BSA in the absence and presence of the quencher (MNPs), respectively. f_a is the fractional maximum FL intensity of BSA, K_{SV} is the quenching constant, and [Q] is the MNPs concentration. As shown in Table 1.

Dynamic quenching depends on diffusion and higher temperature results in larger diffusion coefficient, and the bimolecular quenching constant is expected to be higher with increasing temperature.[18] In contrast, static quenching is dominant when increased temperature results in decreased K_{SV} of the quenching. According to Table 1, the value of K_{SV} decreased with increment of temperature, and thus the quenching process was qualified as static quenching. The static quenching constant (K^θ) of BSA with MNPs could be calculated by the Lineweaver−Burk equation:[22]

$$1/(F_0 - F) = 1/F_0 + 1/(K^\theta F_0[Q]) \quad (3)$$

The value of K^θ decreased with the rise of temperature (Table 2). This indicated that temperature decreased the stability of the complex.[18]

3.2.2. Calculation of Thermodynamic Parameters ΔH^θ, ΔS^θ, and ΔG^θ. The enthalpy of the reaction of MNPs and BSA can be treated as a constant in case there is no remarkable change on temperature. We calculated the enthalpy change (ΔH^θ), free enthalpy change (ΔG^θ), and entropy change (ΔS^θ) according to the following thermodynamic equations:

$$\ln(K_2^\theta/K_1^\theta) = (\Delta H^\theta/R)(1/T_1 - 1/T_2) \quad (4)$$

$$\Delta G^\theta = -RT\ln K^\theta \quad (5)$$

$$\Delta G^\theta = \Delta H^\theta - T\Delta S^\theta \quad (6)$$

R is the gas constant 8.314 J·mol^{-1} ·K^{-1} and T is the temperature (K). K^θ is the equilibrium constant at the corresponding temperature, which stands for static quenching constant in this paper. The values of K^θ, ΔH^θ, ΔS^θ, and ΔG^θ are presented in Table 2. The negative values of ΔG^θ and ΔH^θ reveal spontaneous and exothermic interaction process. The positive entropy change occurred owing to the fact that the H_2O and SDBS molecules coordinated with the MNPs and released at the same time when the MNPs combined with BSA. Furthermore, the increase of the disorder degree obviously proved that the quenching process was static.

3.2.3. Association Constant and Number of Binding Sites. The FL intensities at different concentrations of the BSA−MNPs complexes were analyzed by Scatchard's equation[23] for calculating the association constants:

$$r/C_{Bf} = nK_A - rK_A \quad (7)$$

where r ($r = C_{Bb}/C_{It}$) is the moles of bound BSA per mole of MNPs, C_{Bb} is the molar concentration of bound BSA, C_{Bf} is the molar concentration of free BSA, C_{It} is the total concentration of MNPs. n is the number of binding sites and K_A is the association constant. All experiments were measured at 298 K. As shown in Figure 5, the Scatchard plots were nonlinear, indicating multiple classes of binding sites.[24] We analyzed the

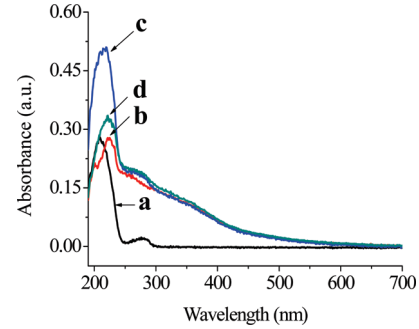

Figure 4. UV−vis absorption spectra of (a) the absorption spectrum of BSA only, (b) the absorption spectrum of MNPs only, (c) the sum of the absorbance of BSA and MNPs, and (d) the absorption spectrum of the mixture (BSA and MNPs). The concentration of MNPs and BSA were fixed at 8.0 × 10^{-9} and 1.0 × 10^{-6} mol·L^{-1}, respectively.

TABLE 2: Lineweaver−Burk Equations and Thermodynamic Parameters for Interaction of MNPs with BSA at 291, 298, and 306 K

T/K	linear equations	K/($\times 10^8$ L·mol^{-1})	r	ΔG^θ/(kJ·mol^{-1})	ΔH^θ/(kJ·mol^{-1})	ΔS^θ/(J·mol^{-1}·K^{-1})
291	$1/(F_0 - F) = 0.037 + 0.15 \times 10^{-9}[Q]^{-1}$	2.42	0.9771	−46.70	−0.90	157.38
298	$1/(F_0 - F) = 0.036 + 0.15 \times 10^{-9}[Q]^{-1}$	2.40	0.9939	−47.80		
306	$1/(F_0 - F) = 0.039 + 0.16 \times 10^{-9}[Q]^{-1}$	2.37	0.9867	−49.06		

high- and low-affinity binding classes only, considering the difficulty of identifying intermediate classes of binding. The high-affinity interaction was estimated at the highest BSA/MNPs concentration ratio, where almost all BSA added were bound to the MNPs, K_A and n were 1.35×10^6 L·mol^{-1} and 284.74, respectively. Moreover, the low-affinity interaction was estimated at the lowest BSA/MNPs ratio. Similarly, almost all BSA-binding sites were occupied, K_A and n were 7.64×10^7 L·mol^{-1} and 46.55, respectively.

3.3. Mechanism. FL quenching may result from a variety of molecular interactions, including excited-state reactions, molecular rearrangements, energy transfer, ground-state complex formation, and collisional quenching.[15,25] A static quenching mechanism for the interaction between BSA and MNPs was suggested in the light of the above results, which might arise from an electrostatic or coordinative interaction.

Raman spectrum is a useful tool to study the interaction of protein and nanoparticles.[26] Figure 6 depicts the Raman spectra of BSA in the absence (Figure 6a) and presence (Figure 6b) of MNPs. The 664.8 and 537 cm^{-1} bands were related to A_{1g}, $T_{2g}(2)$[27] vibration of MNPs, respectively. The 527.3 and 1447.8 cm^{-1} bands were attributed to S−S vibration. The 1000 cm^{-1} wavelength band was related to the α-helix (C−C−N).[28] The band between 1320 and 1340 cm^{-1} was related to the aliphatic lateral chains. Three bands 1620, 1630, and 1690 cm^{-1} were

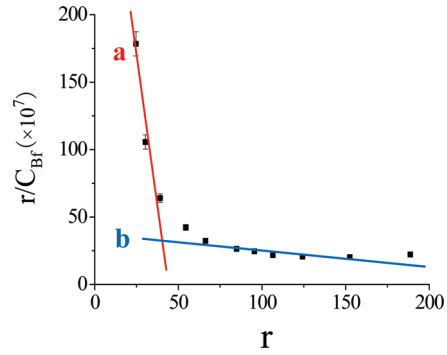

Figure 5. Scatchard plots for the binding of BSA and MNPs at light concentration (a) and high concentration (b) of MNPs.

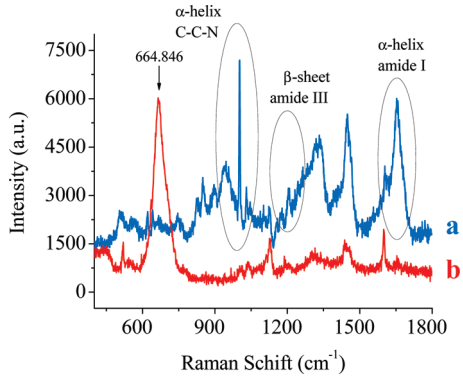

Figure 6. Raman spectra of BSA in the absence (a) and presence (b) of MNPs. The concentrations of BSA and MNPs were 1.0×10^{-5} and 4.0×10^{-7} mol·L^{-1}, respectively.

attributed to antiparallel β-sheet vibrations. The 1654 cm^{-1} band which was mainly contributed from amide I[28] was a characteristic of high α-helical content in BSA. The α-helix structure loss was indicated by intensity diminution at 1654 cm^{-1} band. The 1265 and 1205 cm^{-1} band contributed from amide III. The decreased intensity at 1654 cm^{-1} indicated that the α-helical content in BSA was reduced after binding to MNPs.[29] The 1000 cm^{-1} band related to the phenylalanine and 1345 cm^{-1} band related to tryptophan or C−H bending decreased after BSA interaction with MNPs, showing some structural alterations in the protein conformation.[29] It is well-known that proteins are chains of amino acids where the exact sequence of the amino acids determines the protein's shape, structure, and function. The principal units of protein secondary structure are α-helices and β-sheets, and the three-dimensional arrangement of these is the tertiary structure.[30] Therefore, the presence of MNPs could result in secondary structure alteration in the BSA conformation.

CD spectroscopy is a quantitative technique to investigate the conformation of proteins in aqueous solution.[26] To further investigate the conformation of BSA, CD spectroscopy was performed. The CD spectra (Figure 7) displayed the characteristic peaks (intensive positive peak at around 190 nm and two negative double humped peaks at 208 and 222 nm) of a high α-helical content in native BSA.[31] The fractions of α-helix, β-sheet, turn, and unordered coil are shown in Table 3. Compared to the native BSA, the α-helical content of BSA-MNPs decreased from 55.5 to 47.6%, the β-sheets content increased from 7.6 to 20.4%, and the content of unordered coil decreased from 30.2 to 26.5%. A degree of reduction in the percentage of α-helix (7.9%) and an increase of the β-sheets (12.8%) were observed, which suggested interaction between MNPs and BSA. The decreased percentage of α-helical protein structure indicated that MNPs bound to the amino acid residues

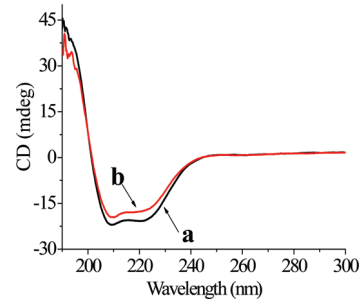

Figure 7. CD spectra of BSA in the absence (a) and presence (b) of MNPs. The concentrations of BSA and MNPs were 2.0×10^{-6} and 2.0×10^{-8} mol·L^{-1}, respectively.

TABLE 3: Fractions of the Secondary Structure of BSA in the Absence and Presence of MNPs[a]

systems	fractions of secondary structure (%)			
	f_α	f_β	f_T	f_U
BSA	55.5	7.6	6.7	30.2
BSA-MNPs	47.6	20.4	5.5	26.5

[a] f_α, f_β, f_T, and f_U are the fractions of α-helix, β-sheet, turn, and unordered coil, respectively.

of the main polypeptide chain of BSA and destroyed the hydrogen bonding networks.[32] This conclusion is in agreement with the results obtained by observation of the Raman spectra.

SDBS ligand was coordinated with MNPs, and it converted hydrophobic MNPs into amphiphilic micelles,[33] which increased hydrophilicity of MNPs. It probably had an inhibiting effect on the interaction between MNPs and BSA. Figure S3 (refer to the Supporting Information) exhibited that there were no obvious changes in relative FL intensity while increasing the concentration of SDBS, which indicated that SDBS had weak inhibiting effect on the interaction between MNPs and BSA. In other words, the coordination was not a dominant factor in the reaction of MNPs with BSA.[8]

The change of ionic strength is an efficient method for distinguishing the binding mode between protein and other molecules. Figure S4 in the Supporting Information depicted the effects of ionic strength on the interaction between BSA and MNPs. With increasing ionic strength of the solution, the decrease of the BSA FL intensity in response to the addition of the same amount of MNPs gradually became smaller, which infers a decrease of quenching efficiency during the binding.[34] The slope of Stern−Volmer plots is actually related to the accessibility (degree of exposure) of the tryptophans to the aqueous quencher.[34] As shown in Figure S4, the slope was smaller at higher concentration of NaCl which eventually implied a reduced accessibility of MNPs to BSA binding sites. The above results indicated that the electrostatic interactions played a key role in the reaction process.[23]

On the basis of the theory of Nemethy and Scheraga,[35] we can infer the main type of interactions between small inorganic molecules and biological macromolecules by enthalpy change (ΔH^{θ}) and entropy change (ΔS^{θ}). So we concluded that the electrostatic force played a key role in the reaction process of MNPs and BSA according to Table 2 ($\Delta H^{\theta} = -0.90$ kJ·mol^{-1} and $\Delta S^{\theta} = 157.38$ J·mol^{-1}·K^{-1}).

4. Conclusion

The interaction between BSA and MNPs was evaluated by the FL, UV−vis, Raman, and CD spectroscopy. A static quenching model based on the quenching rate constants (K_q) and UV−vis absorption spectra was proved reasonably. It was found that the interaction between MNPs and BSA was spontaneous and the electrostatic interactions played key role in the reaction process. The analysis of UV−vis, Raman, and CD spectra indicated that the secondary structure of BSA molecules changed dramatically in the presence of MNPs. Future biological application employing MNPs will be limited by the fact that MNPs have obvious effect on proteins. Therefore, it is imperative that the biocompatibility and biosafety of MNPs should be given more concerns and further studies need to be conducted to achieve a deeper understanding of their biological effect.

Acknowledgment. The authors gratefully acknowledge the support for this research by National Natural Science Foundation of China (20675034), the Program for Academic Pacesetter of Wuhan (200851430484), Nature Science Foundation key project from Hubei Province of China (2008CDA080), the Youth Chengguang Project of Science and Technology of Wuhan City of China (200850731359), and Natural Science Foundation of Hubei Province (No. 2008CDB031).

Supporting Information Available: TGA image and XRD pattern of MNPs, and the effect of different SDBS and NaCl concentrations on the interaction of MNPs with BSA. This material is available free of charge via the Internet at http://pubs.acs.org.

References and Notes

(1) Laurent, S.; Forge, D.; Port, M.; Roch, A.; Robic, C.; Vander Elst, L.; Muller, R. N. *Chem. Rev.* **2008**, *108*, 2064.
(2) AshaRani, P. V.; Mun, G. L. K.; Hande, M. P.; Valiyaveettil, S. *ACS Nano* **2009**, *3*, 279.
(3) Pisanic, T. R.; Blackwell, J. D.; Shubayev, V. I.; Finones, R. R.; Jin, S. *Biomaterials* **2007**, *28*, 2572.
(4) Jeng, H. A.; Swanson, J. *J. Environ. Sci. Health, Part A* **2006**, *41*, 2699.
(5) Wang, Y. Q.; Zhang, H. M.; Zhou, Q. H.; Xu, H. L. *Colloids Surf. A* **2009**, *337*, 102.
(6) Yamasaki, K.; Maruyama, T.; Kragh-Hansen, U.; Otagiri, M. *Biochim. Biophys. Acta* **1996**, *1295*, 147.
(7) Peters, T., Jr. *Adv. Protein Chem.* **1985**, *37*, 161.
(8) Wang, J.; Wang, Y.; Gao, J.; Hu, P.; Guan, H.; Zhang, L.; Xu, R.; Chen, X.; Zhang, X. *Ultrason. Sonochem.* **2009**, *16*, 41.
(9) Kragh-Hansen, U. *Pharmacol. Rev.* **1981**, *33*, 17.
(10) Gnanaprakash, G.; Mahadevan, S.; Jayakumar, T.; Kalyanasundaram, P.; Philip, J.; Raj, B. *Mater. Chem. Phys.* **2007**, *103*, 168.
(11) Lee, H. H.; Yamaoka, S.; Murayama, N.; Shibata, J. *Mater. Lett.* **2007**, *61*, 3974.
(12) Mahadevan, S.; Gnanaprakash, G.; Philip, J.; Rao, B. P. C.; Jayakumar, T. *Physica E* **2007**, *39*, 20.
(13) Huang, J. H.; Parab, H. J.; Liu, R. S.; Lai, T. C.; Hsiao, M.; Chen, C. H.; Sheu, H. S.; Chen, J. M.; Tsai, D. P.; Hwu, Y. K. *J. Phys. Chem. C* **2008**, *112*, 15684.
(14) Gharagozlou, M.; Boghaei, D. M. *Spectrochim. Acta A* **2008**, *71*, 1617.
(15) Shaikh, S. M. T.; Seetharamappa, J.; Ashoka, S.; Kandagal, P. B. *Dyes Pigm.* **2007**, *73*, 211.
(16) Chen, G. Z.; Huang, X. Z.; Xu, J. G.; Zheng, Z. Z.; Wang, Z. B. *The Methods of Fluorescence Analysis*; Beijing Science Press: Beijing 1990; Chapters 1, 2.
(17) Kandagal, P. B.; Seetharamappa, J.; Ashoka, S.; Shaikh, S. M. T.; Manjunatha, D. H. *Int. J. Biol. Macromol.* **2006**, *39*, 234.
(18) Zhang, Y. Z.; Dai, J.; Zhang, X. P.; Yang, X.; Liu, Y. *J. Mol. Struct.* **2008**, *888*, 152.
(19) Glazer, A. N.; Smith, E. L. *J. Biol. Chem.* **1961**, *236*, 2942.
(20) Hu, D. H.; Wu, H. M.; Liang, J. G.; Han, H. Y. *Spectrochim. Acta A* **2008**, *69*, 830.
(21) Eftink, M. R.; Ghiron, C. A. *Biochemistry* **1976**, *15*, 672.
(22) Tian, J.; Liu, J.; He, W.; Hu, Z.; Yao, X.; Chen, X. *Biomacromolecules* **2004**, *5*, 1956.
(23) Zhang, F.; Du, Y.; Ye, B.; Li, P. *J. Photochem. Photobiol. B* **2007**, *86*, 246.
(24) Barbosa, S.; Taboada, P.; Mosquera, V. *Chem. Phys.* **2005**, *310*, 51.
(25) Liang, J.; Cheng, Y.; Han, H. *J. Mol. Struct.* **2008**, *892*, 116.
(26) Shen, X. C.; Liou, X. Y.; Ye, L. P.; Liang, H.; Wang, Z. Y. *J. Colloid Interface Sci.* **2007**, *311*, 400.
(27) Shebanova, O. Comprehensive Summaries of Uppsala Dissertations from the Faculty of Science and Technology, 2003; p 853.
(28) Virgilio, T., Jr.; Parra, D. F.; Polakiewicz, B.; Pitombo, R. N. M. *Int. J. Pharm.* **2005**, *304*, 124.
(29) Meng, G.; Chan, J. C. K.; Rousseau, D.; Li-Chan, E. C.; Y, *J. Agric. Food Chem.* **2005**, *53*, 845.
(30) Lynch, I.; Dawson, K. A. *Nano Today* **2008**, *3*, 40.
(31) Yu, C. H.; Al-Saadi, A.; Shih, S. J.; Qiu, L.; Tam, K. Y.; Tsang, S. C. *J. Phys. Chem. C* **2009**, *113*, 537.
(32) Cheng, X. X.; Lui, Y.; Zhou, B.; Xiao, X. H.; Liu, Y. *Spectrochim. Acta A* **2009**, *72*, 922.
(33) Dubois, F.; Mahler, B.; Dubertret, B.; Doris, E.; Mioskowski, C. *J. Am. Chem. Soc.* **2007**, *129*, 482.
(34) Shang, L.; Jiang, X.; Dong, S. *J. Photochem. Photobiol. A* **2006**, *184*, 93.
(35) Nemethy, G.; Scheraga, H. A. *J. Chem. Phys.* **1962**, *36*, 3382.

JP904004W